



# Shock-Stable Roe Scheme Combining Entropy Fix and Rotated Riemann Solver

Xue-Song Li,\* Xiao-Dong Ren,† Chun-Wei Gu,‡ and Yu-Hong Li‡  
Tsinghua University, 100084 Beijing, People's Republic of China

<https://doi.org/10.2514/1.J058549>

The Roe scheme is an important shock-capturing scheme that is known for its good performance. However, the classical Roe scheme suffers from disastrous problems, such as shock instability for hypersonic flows. The entropy fix and the rotated Riemann solver are common methods used to cure the shock instability. However, these methods may introduce a large and unnecessary numerical dissipation. To cure the shock instability with a minimally increasing numerical dissipation, this study investigates the mechanisms of entropy fix and rotated Roe scheme and combines their complementary advantages. Thus, this paper proposes the Roe-ER scheme, which uses the rotated method to identify where the entropy fix is necessary. Therefore, the possible large dissipation of the rotated Roe scheme is replaced by the relatively small value of entropy fix, and areas that adopt the entropy fix are limited in regions where the shock instability may occur. Numerical cases validate the Roe-ER scheme, which is shock stable, features a low additional numerical dissipation, and can use high-order reconstruction to further reduce areas that activate the entropy fix.

## Nomenclature

$c$	=	speed of sound
$E$	=	total energy
$\mathbf{F}, \mathbf{G}, \mathbf{H}$	=	vectors of the Euler fluxes
$\tilde{\mathbf{F}}$	=	numerical flux
$\tilde{\mathbf{F}}_d$	=	numerical dissipation term
$H$	=	total enthalpy
$\mathbf{n}$	=	face-normal vector
$n_x, n_y, n_z$	=	components of $\mathbf{n}$
$p$	=	pressure
$\mathbf{Q}$	=	vector of conservation variables
$\mathbf{R}$	=	right eigenvector matrices of the governing equations
$u, v, w$	=	velocity components
$x, y, z$	=	Cartesian coordinates
$\rho$	=	fluid density
$\lambda$	=	eigenvalue of the governing equations
$\Lambda$	=	diagonal matrix formed with the relevant eigenvalues
$M$	=	Mach number

## I. Introduction

THE Roe scheme [1] is an important shock-capturing scheme that has undergone considerable development because of its high accuracy and good performance in capturing shock. However, the Roe scheme also features a well-known disastrous shortcoming, that is, the shock instability for the computation of hypersonic flows [2].

The shock instability manifested in different manners, such as the odd-even decoupling for a moving planar shock, a kinked Mach stem for a double-Mach reflection flow, and the carbuncle phenomenon for

a hypersonic blunt body. To address this issue, various methods have been proposed, and these techniques can generally be classified into three groups.

The first group adds a considerable numerical dissipation into the scheme to suppress spurious oscillation and thus stabilize the scheme. Quirk [2] suggested that the Roe scheme can be combined with a highly dissipative scheme, such as the Harten–Lax–van Leer (HLL)-type scheme, through a switch sensor. Another means is the entropy fix, which limits the minimum value of system eigenvalue. The entropy fix is first proposed by Harten and Hyman with a function of the maximum difference of eigenvalues among cell face and left and right sides [3]. Subsequently, the maximum eigenvalue or its relevant variables [4,5] are adopted to better suppress the shock instability. Now, the entropy fix is widely used and has many improved versions [6–10], such as adopting pressure gradient [6] and improvement for triangular grids [8]. Especially, multidimensional characteristics are introduced into the entropy fix by testing all neighboring cell faces [9], testing the Riemann problem for contact and shear waves with an indicator function [10] and so on.

For the second group, the shock instability is caused by the contradiction between the quasi-one-dimensional and grid-aligned characteristics of the scheme and the multidimensional nature of compressible flows. Therefore, the rotated Riemann solvers are proposed for the multidimensional simulations [11,12]. Gas-kinetic theory is another approach used to develop schemes considering the multidimensional characteristics [13–15].

For the last group, the shock instability is due to the pressure difference term in the mass flux of a scheme [16]. Recently, this pressure difference term for all governing equations was further identified as a momentum interpolation method that causes shock instability and should be equal to zero for high-Mach-number flows [17]. Although the term is important, it is not the only factor that produces the shock instability.

To improve the scheme, considering the magnitude of numerical dissipation is important. In fact, the numerical dissipation of Roe scheme seems extremely large for advanced turbulence simulation, such as large-eddy simulation [18,19]. Therefore, exploring the cure for shock instability with minimally increasing numerical dissipation is interesting and necessary.

However, the above-mentioned groups cannot satisfy the requirement. The main disadvantage of the first group method is adding a redundant numerical dissipation. Specifically, although the entropy fix is popular for its simplicity, it introduces an excessive numerical dissipation, and the shock instability is partially cured. For the rotated Roe scheme in the second group, the shock instability can be eliminated, and the numerical dissipation remains unchanged for grid-aligned shear waves. However, the numerical dissipation in

Received 18 April 2019; revision received 27 August 2019; accepted for publication 11 September 2019; published online Open Access 30 September 2019. Copyright © 2019 by the American Institute of Aeronautics and Astronautics, Inc. All rights reserved. All requests for copying and permission to reprint should be submitted to CCC at [www.copyright.com](http://www.copyright.com); employ the eISSN 1533-385X to initiate your request. See also AIAA Rights and Permissions [www.aiaa.org/randp](http://www.aiaa.org/randp).

\*Associate Professor, Key Laboratory for Thermal Science and Power Engineering of Ministry of Education, Department of Energy and Power Engineering; [xs-li@mail.tsinghua.edu.cn](mailto:xs-li@mail.tsinghua.edu.cn) (Corresponding Author).

†Research Assistant, Key Laboratory for Thermal Science and Power Engineering of Ministry of Education, Department of Energy and Power Engineering; [rxid@mail.tsinghua.edu.cn](mailto:rxid@mail.tsinghua.edu.cn).

‡Professor, Key Laboratory for Thermal Science and Power Engineering of Ministry of Education, Department of Energy and Power Engineering; [gcw@mail.tsinghua.edu.cn](mailto:gcw@mail.tsinghua.edu.cn).

certain regions that control shock instability may be extremely large. For the third group, the shock instability can be alleviated to a certain extent by decreasing, rather than increasing, numerical dissipation as expected. However, the problem remains.

This research analyzes the mechanisms of the above-mentioned groups. We find that their advantages can be combined to avoid each group's problems. Therefore, an improved Roe-ER scheme, which combines the entropy fix and the rotated Roe scheme by introducing the method of the third group, is proposed to cure the shock instability with a minimally increasing numerical dissipation.

The remainder of the paper is organized as follows. Section II provides the governing equations and reviews the Roe scheme and its improvements in the three groups. Section III analyzes the entropy fix and the rotated Roe scheme in a uniform framework. Section IV proposes the Roe-ER scheme, and Sec. V provides classical numerical cases to validate the Roe-ER scheme. Finally, Section VI concludes.

## II. Governing Equations and Roe Scheme

### A. Governing Equations

The three-dimensional Navier–Stokes equation can be written as follows:

$$\frac{\partial \mathbf{Q}}{\partial t} + \frac{\partial \mathbf{F}}{\partial x} + \frac{\partial \mathbf{G}}{\partial y} + \frac{\partial \mathbf{H}}{\partial z} = 0 \quad (1)$$

where  $\mathbf{Q} = \begin{bmatrix} \rho \\ \rho u \\ \rho v \\ \rho w \\ \rho E \end{bmatrix}$  is the vector of conservation variables;

$$\mathbf{F} = \begin{bmatrix} \rho u \\ \rho u^2 + p \\ \rho uv \\ \rho uw \\ \rho uH \end{bmatrix}, \mathbf{G} = \begin{bmatrix} \rho v \\ \rho v^2 + p \\ \rho vw \\ \rho vH \end{bmatrix}, \text{ and } \mathbf{H} = \begin{bmatrix} \rho w \\ \rho w^2 + p \\ \rho wH \end{bmatrix} \text{ are}$$

vectors of the Euler fluxes;  $\rho$  denotes fluid density;  $p$  is pressure;  $E$  represents the total energy;  $H$  refers to the total enthalpy; and  $u$ ,  $v$ , and  $w$  correspond to velocity components in Cartesian coordinates, that is,  $(x, y, z)$ , respectively.

### B. Classical Roe Scheme

The classical Roe scheme can be expressed as the sum of a central term and a numerical dissipation term, as shown in the following general form:

$$\tilde{\mathbf{F}} = \frac{1}{2}(\tilde{\mathbf{F}}_L + \tilde{\mathbf{F}}_R) + \tilde{\mathbf{F}}_d \quad (2)$$

where  $\tilde{\mathbf{F}}$  is the numerical flux and  $\tilde{\mathbf{F}}_d$  is the numerical dissipation term. For the cell face in the finite volume method,  $\tilde{\mathbf{F}}$  is given as follows:

$$\tilde{\mathbf{F}} = U \begin{bmatrix} \rho \\ \rho u \\ \rho v \\ \rho w \\ \rho H \end{bmatrix} + p \begin{bmatrix} 0 \\ n_x \\ n_y \\ n_z \\ 0 \end{bmatrix} \quad (3)$$

where  $n_x$ ,  $n_y$ , and  $n_z$  refer to the components of face-normal vector  $\mathbf{n}$ , and  $U = n_x u + n_y v + n_z w$  is the normal velocity on the cell face.

The numerical dissipation term  $\tilde{\mathbf{F}}_d$  is frequently expressed in a vector form as follows:

$$\tilde{\mathbf{F}}_{d,(1/2)}^{\text{Roe}} = -\frac{1}{2} \mathbf{R}_{(1/2)}^{\text{Roe}} \mathbf{\Lambda}_{(1/2)}^{\text{Roe}} (\mathbf{R}_{(1/2)}^{\text{Roe}})^{-1} \Delta \mathbf{Q} \quad (4)$$

where  $\Delta \mathbf{Q} = \mathbf{Q}_R - \mathbf{Q}_L$ , and  $\mathbf{R}^{\text{Roe}}$  is the right eigenvector matrix of the governing equations, and  $\mathbf{\Lambda}^{\text{Roe}}$  is the diagonal matrix formed with the relevant eigenvalues.

$$\lambda_1 = \lambda_2 = \lambda_3 = |U|, \quad \lambda_4 = |U - c|, \quad \lambda_5 = |U + c| \quad (5)$$

where  $c$  is the speed of sound. For simplicity and to avoid confusion, the subscript “1/2” is hereafter omitted.

### C. Entropy Fix

When one eigenvalue in Eq. (5) tends to zero, the large discrepancy among eigenvalues renders the system of the Navier–Stokes equation rigid. To address this issue, the entropy fix is adopted to prevent small eigenvalues. A commonly used version changes the eigenvalues in Eq. (5) as follows:

$$\lambda_i = \begin{cases} \lambda_i, & \lambda_i \geq h, \\ \frac{1}{2} \left( \frac{\lambda_i^2}{h} + h \right), & \lambda_i < h \end{cases} \quad (6)$$

$$h = \varepsilon_\lambda \max(\lambda_i) = \varepsilon_\lambda (|U| + c) \quad (7)$$

where  $\varepsilon_\lambda$  is a constant with a frequently adopted value of 0.05–0.2. Equations (6) and (7) are a simple version of the entropy fix [4]. It is adopted in this paper because it is easy to observe its relation with the rotated Roe scheme and it performs well enough for the Roe-ER scheme.

### D. Rotated Roe Scheme

For the Roe scheme, the numerical dissipation term  $\tilde{\mathbf{F}}_d$  is constructed on the basis of the grid-aligned direction of the cell-face normal vector  $\mathbf{n}$ , as shown in Eqs. (4) and (5). For the rotated Roe scheme [11], direction  $\mathbf{n}$  is replaced by two vertical vectors, namely,  $\mathbf{n}_1$  and  $\mathbf{n}_2$ , which are based on physical flows rather than the grid. Therefore, the numerical dissipation term of the rotated Roe scheme is given as follows:

$$\tilde{\mathbf{F}}_d^{\text{Rot}} = -\frac{1}{2} [|\alpha_1| \mathbf{R}_1 \mathbf{\Lambda}_1 (\mathbf{R}_1)^{-1} + |\alpha_2| \mathbf{R}_2 \mathbf{\Lambda}_2 (\mathbf{R}_2)^{-1}] \Delta \mathbf{Q} \quad (8)$$

where  $\mathbf{R}_1$ ,  $\mathbf{\Lambda}_1$ ,  $\mathbf{R}_2$ , and  $\mathbf{\Lambda}_2$  are the right eigenvector and diagonal matrixes of eigenvalues based on  $\hat{\mathbf{n}}_1$  and  $\hat{\mathbf{n}}_2$ , respectively.  $\hat{\mathbf{n}}_1$  and  $\hat{\mathbf{n}}_2$  are the normalized unit vectors that correspond to  $\mathbf{n}_1$  and  $\mathbf{n}_2$  as follows:

$$\hat{\mathbf{n}}_1 = \text{sign}(\alpha_1) \mathbf{n}_1 \quad (9)$$

$$\hat{\mathbf{n}}_2 = \text{sign}(\alpha_2) \mathbf{n}_2 \quad (10)$$

and

$$\alpha_1 = \mathbf{n}_1 \cdot \mathbf{n} \quad (11)$$

$$\alpha_2 = \mathbf{n}_2 \cdot \mathbf{n} \quad (12)$$

## III. Mechanism Analysis of Roe-Type Schemes

### A. Uniform Framework

The numerical dissipation term in Eq. (4) can also be expressed as an equivalent scale algorithm [20,21] as follows:

$$\tilde{\mathbf{F}}_d = -\frac{1}{2} \left\{ \xi \begin{bmatrix} \Delta \rho \\ \Delta(\rho u) \\ \Delta(\rho v) \\ \Delta(\rho w) \\ \Delta(\rho E) \end{bmatrix} + (\delta p_u + \delta p_p) \begin{bmatrix} 0 \\ n_x \\ n_y \\ n_z \\ U \end{bmatrix} + (\delta U_u + \delta U_p) \begin{bmatrix} \rho \\ \rho u \\ \rho v \\ \rho w \\ \rho H \end{bmatrix} \right\} \quad (13)$$

where  $\xi$  is the basic upwind dissipation,  $\delta p_p$  is the pressure-difference-driven modification for the cell face pressure,  $\delta p_u$  denotes velocity-difference-driven modifications for the cell face pressure,  $\delta U_u$  indicates the velocity-difference-driven modification for the cell face velocity, and  $\delta U_p$  specifies the pressure-difference-driven modification for cell face velocity.

Equation (13) can be regarded as a uniform framework for the shock-capturing scheme [21], which is simple, computationally inexpensive, and easy to analyze and improve. Therefore, Eq. (13) serves as the basis of this work.

### B. Classical Roe Scheme

On the basis of Eq. (13), the classical Roe scheme is expressed as follows:

$$\xi = \lambda_1 \quad (14)$$

$$\delta p_u = \left( \frac{\lambda_5 + \lambda_4}{2} - \lambda_1 \right) \rho \Delta U \quad (15)$$

$$\delta p_p = \frac{\lambda_5 - \lambda_4}{2} \frac{\Delta p}{c} \quad (16)$$

$$\delta U_u = \frac{\lambda_5 - \lambda_4}{2} \frac{\Delta U}{c} \quad (17)$$

$$\delta U_p = \left( \frac{\lambda_5 + \lambda_4}{2} - \lambda_1 \right) \frac{\Delta p}{\rho c^2} \quad (18)$$

On the basis of Eq. (5), Eqs. (14)–(18) can be further simplified as follows:

$$\xi = |U| \quad (19)$$

$$\delta p_u = \max(0, c - |U|) \rho \Delta U \quad (20)$$

$$\delta p_p = \text{sign}(U) \min(|U|, c) \frac{\Delta p}{c} \quad (21)$$

$$\delta U_u = \text{sign}(U) \min(|U|, c) \frac{\Delta U}{c} \quad (22)$$

$$\delta U_p = \max(0, c - |U|) \frac{\Delta p}{\rho c^2} \quad (23)$$

### C. Method of the Third Group

In relation to the method of the third group, as discussed in Sec. I, the pressure difference term should be equal to zero for high-Mach-number flows [17]. That is,

$$\delta U_p = 0 \quad (24)$$

Equation (24) can prevent the destruction of physical compression shock to a considerable extent. However, it deteriorates the nonphysical expansion shock and renders the traditional curing method for the expansion shock invalid. Therefore, Ref. [22] proposed an improved method, which replaces  $|U|$  in terms  $\delta p_p$ ,  $\delta p_u$ , and  $\delta U_u$  with  $|U|'$  defined as follows:

$$|U|' = |U| - \frac{\text{sign}(U + c) \max(0, U_R - U_L) - \text{sign}(U - c) \max(0, U_R - U_L)}{4} \quad (25)$$

If  $U$  is defined as follows:

$$U = \frac{U_R + U_L}{2} \quad (26)$$

then Eq. (25) can also be expressed as follows:

$$|U|' = \begin{cases} \min(|U_L|, |U_R|) & |U| < c \text{ and } U_R > U_L \\ |U| & \text{otherwise} \end{cases} \quad (27)$$

Thus, the value of  $|U|'$  decreases within a reasonable range for subsonic expansion flows. Then,  $\delta p_u$  increases, and  $\delta p_p$  and  $\delta U_u$  decrease synchronously. This improvement is effective for suppressing expansion shock.

The expansion shock occurs when  $|U| \rightarrow c$ . To minimize the impact of extra modification, Eq. (25) can be further improved as follows:

$$|U|' = |U| - f^8(\bar{M}) \times \frac{\text{sign}(U + c) \max(0, U_R - U_L) - \text{sign}(U - c) \max(0, U_R - U_L)}{4} \quad (28)$$

$$f(M) = \min \left( M \frac{\sqrt{4 + (1 - M^2)^2}}{1 + M^2}, 1 \right) \quad (29)$$

where  $\bar{M} = |U|/c$  and the purpose of the function  $f^8$  is to obtain smooth transitions near 0 and 1 of the Mach number.

### D. Entropy Fix

The entropy fix is activated when  $|U| \rightarrow 0$  or  $|U| \rightarrow c$ . For the condition of  $|U| \rightarrow c$ , the entropy fix plays the role of suppressing expansion shock. For this function, however, the entropy fix can be replaced by Eq. (28) with a less dissipation. Therefore, we focus only on the condition of  $|U| \rightarrow 0$  as follows.

When  $|U| \rightarrow 0$ , the entropy fix suppresses shock instability. For this condition, the entropy fix changes the terms  $\xi$ ,  $\delta p_u$ , and  $\delta U_p$  compared with the classical Roe scheme, which is based on Eqs. (13)–(18).

$$\xi \approx \varepsilon_\lambda c \quad (30)$$

$$\delta p_u \approx \max(0, 1 - \varepsilon_\lambda) \rho c \Delta U \quad (31)$$

$$\delta U_p \approx \max(0, 1 - \varepsilon_\lambda) \frac{\Delta p}{\rho c} \quad (32)$$

The effect of entropy fix can be neglected for the terms  $\delta p_u$  and  $\delta U_p$  because  $\varepsilon_\lambda$  is small compared with 1. Therefore, the mechanism of suppressing the shock instability of entropy fix is attributed to the increase in the term for the basic upwind dissipation, that is,  $\xi$ .

### E. Rotated Roe Scheme

The rotated Roe scheme can also be expressed in the form of Eq. (13) as follows:

$$\xi = U_{\text{rot}} = |\alpha_1 U_1| + |\alpha_2 U_2| \quad (33)$$

$$\delta p_u = |\alpha_1| \max(0, c - |U_1|) \rho \Delta U_1 \begin{bmatrix} 0 \\ n_{x1}/n_x \\ n_{y1}/n_y \\ n_{z1}/n_z \\ U_1/U \end{bmatrix} + |\alpha_2| \max(0, c - |U_2|) \rho \Delta U_2 \begin{bmatrix} 0 \\ n_{x2}/n_x \\ n_{y2}/n_y \\ n_{z2}/n_z \\ U_2/U \end{bmatrix} \quad (34)$$

$$\delta p_p = |\alpha_1| \text{sign}(U_1) \min(|U_1|, c) \frac{\Delta p}{c} \begin{bmatrix} 0 \\ n_{x1}/n_x \\ n_{y1}/n_y \\ n_{z1}/n_z \\ U_1/U \end{bmatrix} + |\alpha_2| \text{sign}(U_2) \min(|U_2|, c) \frac{\Delta p}{c} \begin{bmatrix} 0 \\ n_{x2}/n_x \\ n_{y2}/n_y \\ n_{z2}/n_z \\ U_2/U \end{bmatrix} \quad (35)$$

$$\delta U_u = |\alpha_1| \text{sign}(U_1) \min(|U_1|, c) \frac{\Delta U_1}{c} + |\alpha_2| \text{sign}(U_2) \min(|U_2|, c) \frac{\Delta U_2}{c} \quad (36)$$

$$\delta U_p = |\alpha_1| \max(0, c - |U_1|) \frac{\Delta p}{\rho c^2} + |\alpha_2| \max(0, c - |U_2|) \frac{\Delta p}{\rho c^2} \quad (37)$$

where

$$U_1 = \text{sign}(\alpha_1)(\hat{n}_{1x}u + \hat{n}_{1y}v + \hat{n}_{1z}w) \quad (38)$$

$$U_2 = \text{sign}(\alpha_2)(\hat{n}_{2x}u + \hat{n}_{2y}v + \hat{n}_{2z}w) \quad (39)$$

To analyze the mechanism of the rotated Roe scheme, two typical conditions are given.

- 1) The condition of  $|\alpha_1| = |\alpha_2| = |\alpha| = (\sqrt{2}/2)$ , as shown in Fig. 1a,  $|U_1| = |U_2| = (\sqrt{2}/2)V$ , where  $V = \sqrt{u^2 + v^2 + w^2}$  is the flow velocity with its direction parallel to the cell face.

As discussed in Eqs. (24) and (30), the terms  $\xi$  and  $\delta U_p$  play important roles for the shock instability. In fact, the terms  $\delta p_u$ ,  $\delta p_p$ , and  $\delta U_u$  have little effect on the shock instability. Therefore, we focus only on the terms  $\xi$  and  $\delta U_p$  for this condition.

For the classical Roe scheme,

$$\xi = 0 \quad (40)$$

$$\delta U_p = \frac{\Delta p}{\rho c} \quad (41)$$

For the rotated Roe scheme, as shown in Fig. 1a:

$$\xi = U_{\text{rot}} = V \quad (42)$$

$$\delta U_p = \max(0, \sqrt{2}c - |V|) \frac{\Delta p}{\rho c^2} \quad (43)$$

For supersonic flows  $M \geq \sqrt{2}$ , Eq. (43) becomes Eq. (24). Therefore, for certain rotated directions, the rotated Roe scheme introduces the mechanism of the third group and an extremely large dissipation term, namely,  $\xi$ , which is larger than that of the entropy fix in Eq. (30).

- 2) The condition of  $|\alpha_1| = 0$  and  $|\alpha_2| = 1$  (i.e.,  $\mathbf{n}_1$  is parallel to the cell face, as shown in Fig. 1b), or  $|\alpha_1| = 1$  and  $|\alpha_2| = 0$  (i.e.,  $\mathbf{n}_1$  is parallel to the normal cell face, as shown in Fig. 1c).

For this condition, the terms of the rotated Roe scheme in Eqs. (33–37) recover a state similar to that of the classical Roe scheme [Eqs. (19–23)]. Therefore, for waves that are parallel or vertical to the cell face, the rotated Roe scheme maintains accuracy similar to that of the classical Roe scheme.

The previous discussions demonstrate the importance of determining  $\mathbf{n}_1$ . Reference [11] provides a good option based on the direction of velocity difference.

#### IV. Improvement of Roe-ER Schemes

Section III demonstrated that the rotated Roe scheme can hold the accuracy of the classical Roe scheme for required areas and provide substantial mechanisms that suppress the shock instability by introducing the mechanism of the third group and a large term  $\xi$ . However,  $\xi$  seems largely dissipative. From another angle, the role of entropy fix is also reflected in  $\xi$ , where the term  $\xi$  of entropy fix is much smaller than that of the rotated Roe scheme. However, it exists whether or not it is necessary.

Therefore, the complementary advantages of the three methods for curing shock instability, especially for the rotated Roe scheme and entropy fix, can be combined. Thus, the Roe-ER scheme is proposed as follows:

$$\xi = \max[|U|, \min(U_{\text{ef}}, U_{\text{rot}})] \quad (44)$$

$$\delta p_u = \max(0, c - |U|') \rho \Delta U \quad (45)$$

$$\delta p_p = \text{sign}(U) \min(|U|', c) \frac{\Delta p}{c} \quad (46)$$

$$\delta U_u = \text{sign}(U) \min(|U|', c) \frac{\Delta U}{c} \quad (47)$$

$$\delta U_p = 0 \quad (48)$$

where  $|U|'$  is used to avoid the expansion shock.

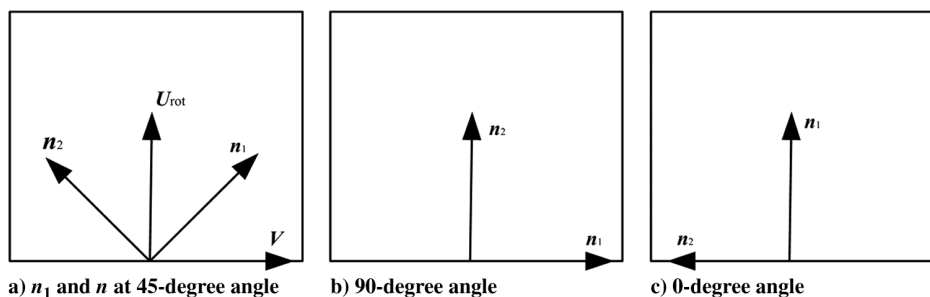


Fig. 1 Typical conditions of the rotated Roe scheme.

$$|U|' = |U| - \frac{\text{sign}(U + c) \max(0, U_R - U_L) - \text{sign}(U - c) \max(0, U_R - U_L)}{4} \quad (49)$$

where  $U_{\text{ef}}$  is the velocity corresponding to the entropy fix.

$$U_{\text{ef}} = \varepsilon c \quad (50)$$

where  $\varepsilon$  is a small constant and  $U_{\text{rot}}$  is the rotated normal velocity on the cell face.

$$U_{\text{rot}} = |\alpha_1 U_1| + |\alpha_2 U_2| \quad (51)$$

$$U_1 = \mathbf{n}_1 \cdot \mathbf{V} \quad (52)$$

$$U_2 = \mathbf{n}_2 \cdot \mathbf{V} \quad (53)$$

$$\alpha_1 = \mathbf{n}_1 \cdot \mathbf{n} \quad (54)$$

$$\alpha_2 = \mathbf{n}_2 \cdot \mathbf{n} \quad (55)$$

$$\mathbf{n}_2 = (\mathbf{n}_1 \times \mathbf{n}) \times \mathbf{n}_1 \quad (56)$$

$$\mathbf{V} = u\mathbf{i} + v\mathbf{j} + w\mathbf{k} \quad (57)$$

and  $\mathbf{n}_1$  are selected based on the direction of velocity difference [11] as follows:

$$\mathbf{n}_1 = \begin{cases} \mathbf{n} & \text{if } \Delta V = \sqrt{(\Delta u)^2 + (\Delta v)^2 + (\Delta w)^2} < \delta \\ \frac{\Delta u\mathbf{i} + \Delta v\mathbf{j} + \Delta w\mathbf{k}}{V} & \text{otherwise} \end{cases} \quad (58)$$

Reference [11] defines  $\delta$  as an extremely small positive value. This paper considers that the rotated method focuses only on shock. Thus, velocity jump  $\Delta V$  is limited by a relatively large value as follows:

$$\delta = 0.01c \quad (59)$$

That is to say, the rotated method is activated only when flow fields change to a certain extent, else  $U_{\text{rot}} = U$ .

The Roe-ER scheme changes  $\xi$ , which can also be expressed as follows:

$$\xi = \begin{cases} U_{\text{ef}} & \text{when } U_{\text{ef}} < U_{\text{rot}} \text{ and } U_{\text{ef}} > |U| \\ U_{\text{rot}} & \text{when } U_{\text{rot}} < U_{\text{ef}} \text{ and } U_{\text{rot}} > |U| \\ |U| & \text{otherwise} \end{cases} \quad (60)$$

Then, the maximum fix value that replaces  $|U|$  is  $\varepsilon c$  by the entropy fix, which prevents excessive dissipation by the rotated method for shock areas. When  $U_{\text{rot}} < U_{\text{ef}}$ , the entropy fix is replaced by  $U_{\text{rot}}$  or  $|U|$ , which prevents excessive dissipation for shear waves by entropy fix. The value of  $\xi$  is in general equal to  $|U|$  or  $U_{\text{ef}}$  because condition  $U_{\text{rot}} < U_{\text{ef}}$  and  $U_{\text{rot}} > |U|$  is scarcely met.

Additionally, the Roe-ER scheme eliminates an important source that activates the shock instability by setting  $\delta U_p = 0$ . Thus,  $\varepsilon$  can be relatively smaller than that of the classical entropy fix to suppress shock instability.

Like the classical Roe scheme, the Roe-ER scheme can be combined with any space reconstruction method. It is first-order accuracy with a zero-order reconstruction as follows:

$$\phi_{j+(1/2),L} = \phi_j \quad (61)$$

$$\phi_{j+(1/2),R} = \phi_{j+1} \quad (62)$$

where  $\phi$  represents anyone of the conservation variables.

For high-order accuracy, in this paper the known monotone upstream-centered schemes for conservation laws (MUSCL reconstruction) with the minmod limiter for the TVD characteristic (MUSCL-TVD) are adopted because they are extensively used. The MUSCL-TVD reconstruction method is described as follows:

$$\phi_{j+(1/2),L} = \phi_j + \frac{1}{4}[(1 - \varpi)\bar{\bar{\delta}}\phi_{j-(1/2)} + (1 + \varpi)\bar{\bar{\delta}}\phi_{j+(1/2)}] \quad (63)$$

$$\phi_{j+(1/2),R} = \phi_{j+1} - \frac{1}{4}[(1 - \varpi)\bar{\bar{\delta}}\phi_{j+(3/2)} + (1 + \varpi)\bar{\bar{\delta}}\phi_{j+(1/2)}] \quad (64)$$

where  $\varpi = (1/3)$ , and

$$\bar{\bar{\delta}}\phi_{j+(1/2)} = \varphi(\delta\phi_{j+(1/2)}, \bar{\bar{\omega}}\delta\phi_{j-(1/2)}) \quad (65)$$

$$\bar{\bar{\delta}}\phi_{j+(1/2)} = \varphi(\delta\phi_{j+(1/2)}, \bar{\bar{\omega}}\delta\phi_{j+(3/2)}) \quad (66)$$

where  $\bar{\bar{\omega}} = 1$  and  $\varphi$  is a limiter. For the minmod limiter,

$$\varphi(a, b) = \text{sign}(a) \cdot \max[0, \min(|a|, \text{sign}(a) \cdot b)] \quad (67)$$

## V. Numerical Tests

For the following cases, the three-stage TVD Runge–Kutta scheme is adopted for time discretization. For space discretization, the first-order accuracy with Eqs. (61) and (62) is adopted to discuss the schemes themselves, and the MUSCL-TVD reconstruction with Eqs. (63–67) is also adopted to discuss the performance of high-order accuracy. For simplicity, in the following text the scheme names mean first-order accuracy unless specifically specified as the MUSCL-TVD reconstruction.

For all numerical tests,  $\varepsilon = 0.05$  in Eq. (50), which indicates that a low additional numerical dissipation of  $U_{\text{ef}} = 0.05c$  is enough for almost all conditions to remain shock stable when the Roe-ER scheme is adopted.

### A. Odd–Even Decoupling Test

The odd–even decoupling test is an important case designed by Quirk [2], because any scheme that suffers it also suffers from shock instability in other classical cases. The initial conditions are given as  $(\rho, p, u, v)_L = ((1512/205), (251/6), (175/36), 0)$  and  $(\rho, p, u, v)_R = (1.4, 1, 0, 0)$ . Therefore, a planar shock moves with a Mach number of 6 in a duct. The computational mesh includes  $20 \times 800$  right orthogonal uniform grids in the  $Y$  and  $X$  directions, except that the centerline grid is odd–even disturbed as follows:

$$Y_{i,j,\text{mid}} = \begin{cases} Y_{j,\text{mid}} + \varepsilon_y \Delta Y, & \text{for } i \text{ even,} \\ Y_{j,\text{mid}} - \varepsilon_y \Delta Y, & \text{for } i \text{ odd} \end{cases} \quad (68)$$

In this test, a large value of  $\varepsilon_y = 0.1$  is adopted because it produces a severe odd–even decoupling compared with small values.

Figure 2a shows that the classical Roe scheme smoothens and destroys moving shock at 100 s. After adopting entropy fix [Eqs. (6) and (7)], the result achieves only a minor improvement with  $\varepsilon_\lambda = 0.05$ , and shock is seriously deformed even when  $\varepsilon_\lambda = 0.2$ , as shown in Figs. 2b and 2c.

Adopting the classical Roe scheme with Eq. (48),  $\delta U_p = 0$ , and as shown in Fig. 2d, shock instability is also severe but better than that obtained by the classical Roe scheme. Shock instability is cured by further introducing the improvement for the term  $\xi$  in Eq. (44), that is, adopting the Roe-ER scheme, as shown in Fig. 2e. By MUSCL-TVD reconstruction, the high-order Roe-ER scheme can also obtain a

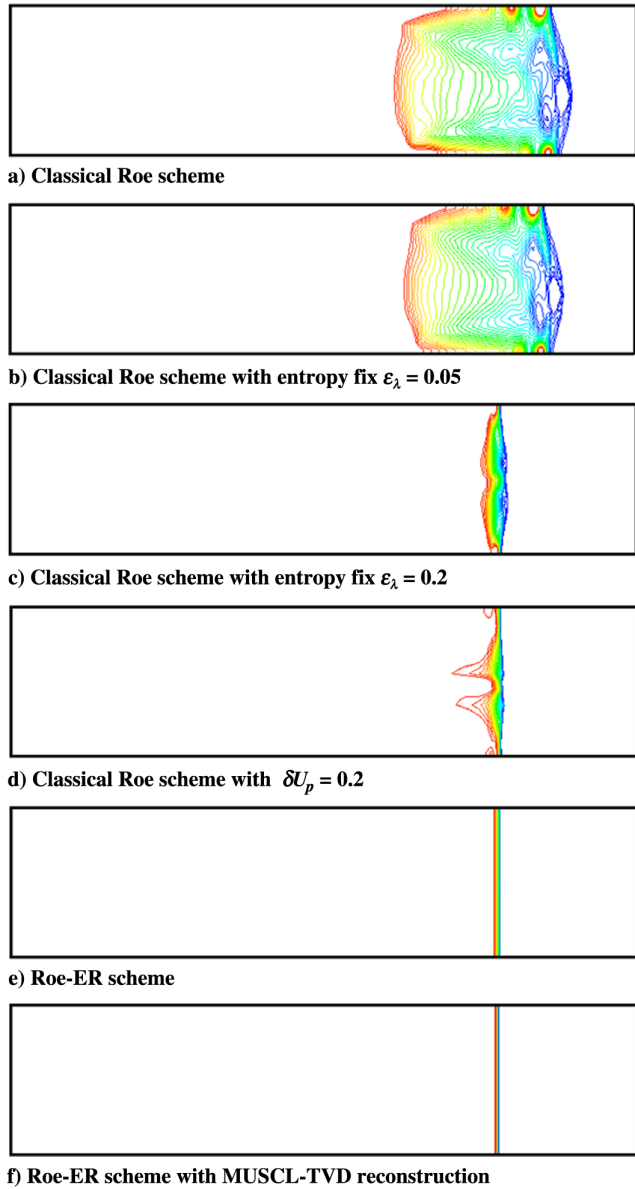


Fig. 2 Density contours of odd-even decoupling test at  $t = 100$  s.

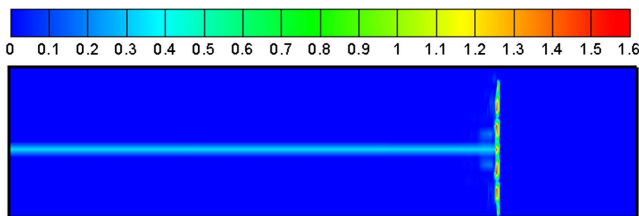


Fig. 3 Contours of rotated Mach number  $M_{\text{rot}} = U_{\text{rot}}/c$  on cells parallel to flows.

shock-stable solution with improved shock resolution, as shown in Fig. 2f.

Based on the results in Fig. 2e, Fig. 3 shows contours of the rotated Mach number  $M_{\text{rot}} = U_{\text{rot}}/c$  on cell faces parallel to the  $X$  direction, where  $U = 0$  in theory except for odd-even disturbed centerline cell faces. Clearly, the rotated Mach number is nearly zero on the smooth area, which is better than the result for entropy fix.  $M_{\text{rot}}$  values are activated around the shock and disturbed centerline faces, with large and maximum values up to 1.6. Such values seem extremely large, although they render the scheme highly robust. Figure 3 explains the

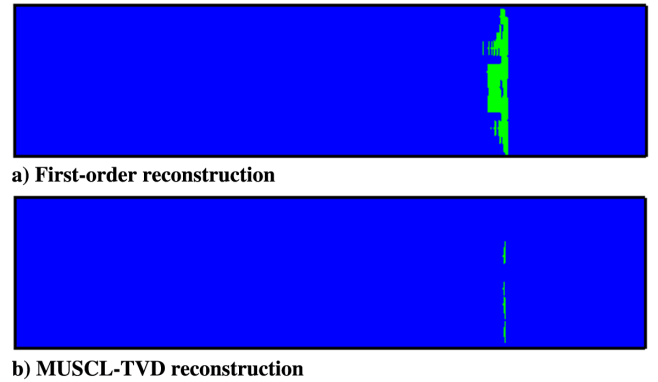


Fig. 4 Contours of function  $I_d$  after identifying areas of entropy fix.

complementary advantages of entropy fix and the rotated Riemann solver.

In Fig. 4, a function, namely,  $I_d$ , is defined as follows:

$$I_d = \begin{cases} 1 & \text{when } U_{\text{ef}} < U_{\text{rot}} \text{ and } U_{\text{ef}} > |U| \\ 0 & \text{otherwise} \end{cases} \quad (69)$$

This function is adopted to identify the area in which the entropy fix takes effect. Figure 4a shows that the working area of the entropy fix is small and located on the region where shock instability possibly occurs. Adopting the MUSCL-TVD reconstruction, this working area is reduced to nearly invisible, as shown in Fig. 4b. Figure 4 demonstrates that the Roe-ER scheme achieves the goal of limiting the entropy fix in its necessary area. Thus, entropy fix holds a shock-stable advantage and has little effect on scheme accuracy.

## B. Supersonic Corner Test

The supersonic corner test considers a moving supersonic shock around a  $90^\circ$  corner. In addition to shock instability, an expansion shock may be produced through numerical computation around the corner in which a series of expansion waves exist.

The initial conditions of the supersonic corner test are as follows:  $\rho_L = 7.04108$ ,  $u_L = 4.07794$ ,  $v_L = 0$ ,  $p_L = 30.05942$ ,  $\rho_R = 1.4$ ,  $u_R = v_R = 0$ , and  $p_R = 1$  at the  $x$ -axis position of 0.05. With  $400 \times 400$  grids, the classical Roe scheme produces instability at the top right corner of the shock, as shown in Fig. 5a. Adopting the entropy fix with a large value of  $\varepsilon_\lambda = 0.2$ , instability is improved but remains obvious, as shown in Fig. 5b. Adopting the classical Roe scheme with  $\delta U_p = 0$ , the shock instability in Fig. 5c is similar to that in Fig. 5b, and a visible expansion shock occurs.

Adopting the Roe-ER scheme, shock instability and expansion shock are simultaneously fixed as expected (Fig. 5d). Considering MUSCL-TVD reconstruction, the result shown in Fig. 5e is better than that in Fig. 5d.

Figure 6 shows the areas of activated entropy fix by the identification function  $I_d$ . Figure 6a shows that the entropy fix takes effect only on small areas around the shock and beginning and end of expansion waves. The main activated areas are concentrated in the top shock, where shock instability occurs. Adopting the MUSCL-TVD reconstruction, the activated areas are further reduced, as shown in Fig. 6b, which indicates that the influence of entropy fix is reduced for high-order accuracy as we expected.

## C. Kinked Mach Stem of Double-Mach Reflection Test

The kinked Mach stem of the double-Mach reflection test is another well-known shock instability problem. This problem occurs when an inclined moving shock is reflected from a wall. Shock is initially set up at an inclination angle of  $60^\circ$  with a Mach number of 10.

Figure 7 shows density contours at 0.2 s on  $200 \times 800$  grids. For the classical Roe scheme, shock is severely deformed, and a nonphysical triple point appears. These conditions make up the

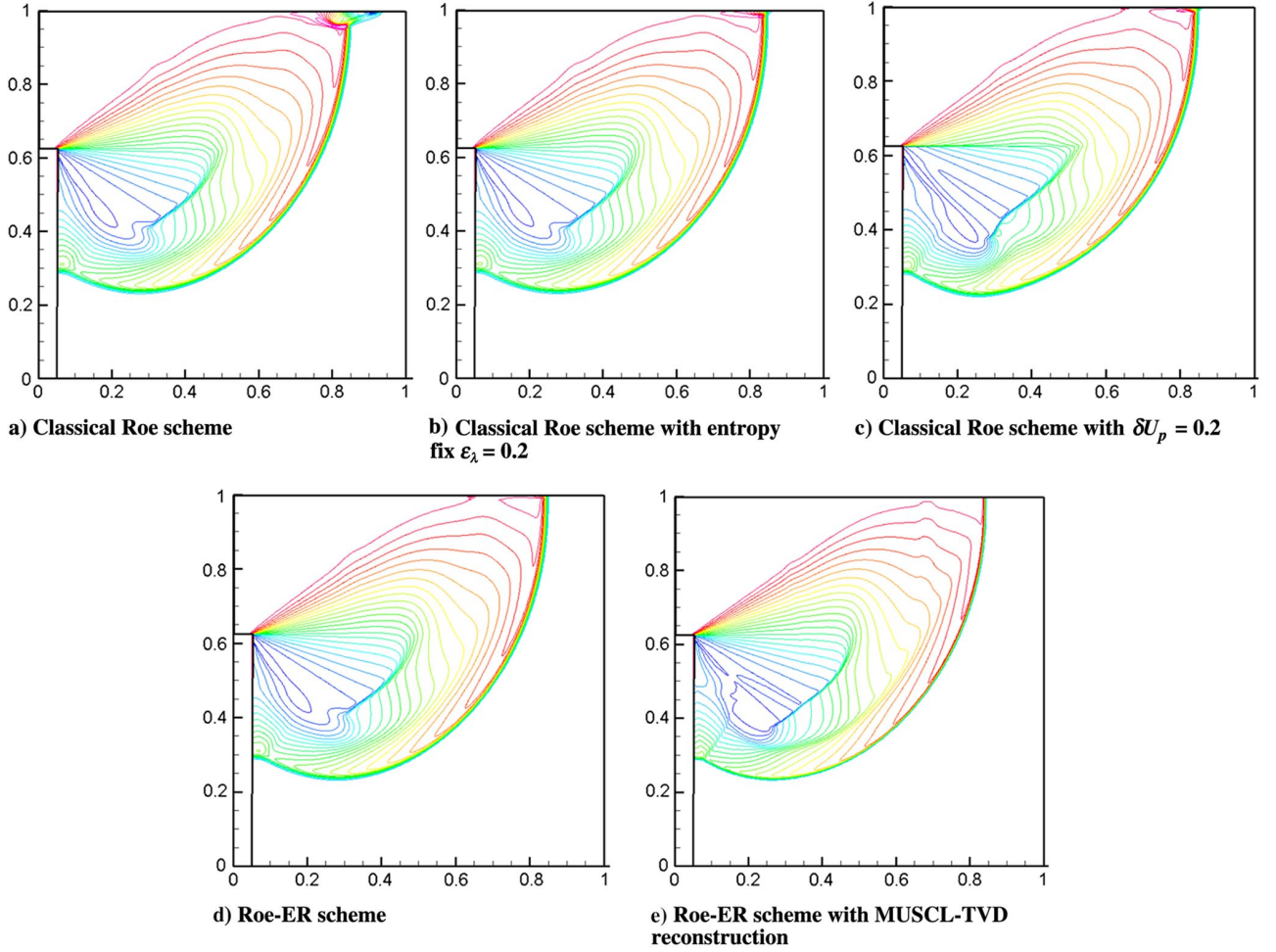


Fig. 5 Density contours of supersonic corner test at  $t = 0.155$  s.

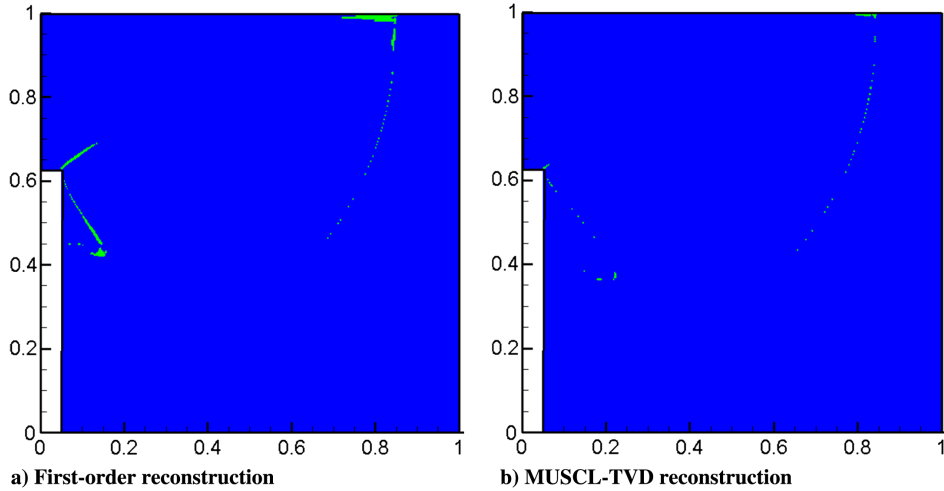


Fig. 6 Contours of function  $I_d$  after identifying areas of entropy fix.

kinked Mach stem, as shown in Fig. 7a. As expected, for the Roe-ER scheme without and with the MUSCL-TVD reconstruction, the kinked Mach stems are fixed in Figs. 7b and 7c, respectively. Figure 8 also shows the activated areas of entropy fix, which are small and can be further reduced by high-order reconstruction.

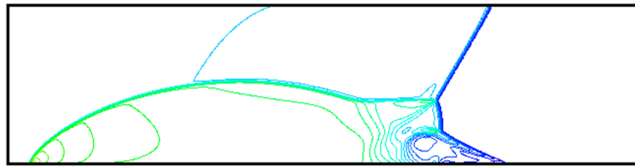
## VI. Conclusions

This paper investigated the mechanisms of entropy fix and the rotated Roe for curing the shock instability as follows:

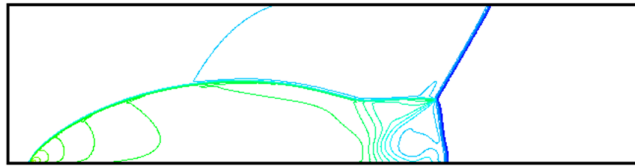
- 1) The entropy fix increases the basic upwind dissipation term  $\xi$  by limiting its minimal value.
- 2) The rotated Roe scheme increases the term  $\xi$  up to the local velocity and can decrease the term  $\delta U_p$  to zero.
- 3) The entropy fix and the rotated Roe scheme can be combined with complementary advantages, that is, adopting the rotated  $\xi$  term to identify where the entropy fix is necessary.

Therefore, the shock-stable Roe-ER scheme is proposed, which improves the construction of the term  $\xi$  and renders  $\delta U_p = 0$ . Numerical cases validate that the Roe-ER scheme can effectively

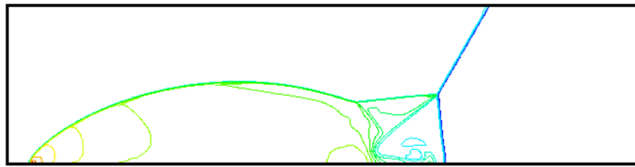




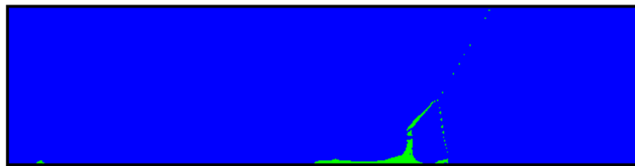
a) Classical Roe scheme



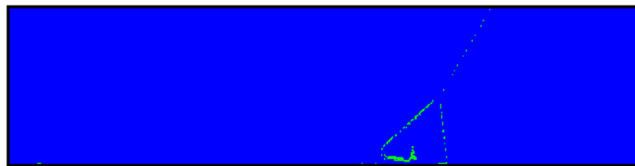
b) Roe-ER scheme



c) Roe-ER scheme with MUSCL-TVD reconstruction

Fig. 7 Density contours of the double-Mach reflection test at  $t = 0.2$  s.

a) First-order reconstruction



b) MUSCL-TVD reconstruction

Fig. 8 Contours of function  $I_d$  after identifying areas of entropy fix.

suppress the shock instability. The additional numerical dissipation is low, because the value itself of entropy fix is small, and the areas that activate the entropy fix are mainly distributed in regions where the shock instability may occur and can be further reduced by the high-order MUSCL-TVD reconstruction. Therefore, the Roe-ER scheme achieves the aim of curing shock instability with a minimally increasing numerical dissipation.

### Acknowledgment

This study was supported by the National Science and Technology Major Project of China (2017-II-0006-0020).

### References

- [1] Roe, P. L., "Approximate Riemann Solvers: Parameter Vectors and Difference Schemes," *Journal of Computational Physics*, Vol. 43, No. 2, 1981, pp. 357–372.  
[https://doi.org/10.1016/0021-9991\(81\)90128-5](https://doi.org/10.1016/0021-9991(81)90128-5)
- [2] Quirk, J. J., "A Contribution to the Great Riemann Solver Debate," *International Journal for Numerical Methods in Fluids*, Vol. 18, No. 6, 1994, pp. 555–574.  
[https://doi.org/10.1002/\(ISSN\)1097-0363](https://doi.org/10.1002/(ISSN)1097-0363)
- [3] Harten, A., and Hyman, J. M., "Self-Adjusting Grid Methods for One-Dimensional Hyperbolic Conservation Laws," *Journal of Computational Physics*, Vol. 50, No. 2, 1983, pp. 235–269.  
[https://doi.org/10.1016/0021-9991\(83\)90066-9](https://doi.org/10.1016/0021-9991(83)90066-9)
- [4] Yee, H. C., "Upwind and Symmetric Shock-Capturing Schemes," NASA TM-89464, May 1987.
- [5] Muller, B., "Simple Improvements If an Upwind TVD Scheme for Hypersonic Flow," AIAA Paper 1989-1977, 1989.  
<https://doi.org/10.2514/6.1989-1977>
- [6] Lin, H. C., "Dissipation Addition to Flux-Difference Splitting," *Journal of Computational Physics*, Vol. 117, No. 1, 1995, pp. 20–27.  
<https://doi.org/10.1006/jcph.1995.1040>
- [7] Kermani, M. J., and Plett, E. G., "Modified Entropy Correction Formula for the Roe Scheme," AIAA Paper 2001-0083, Jan. 2001.
- [8] Dechaumphai, P., and Phongthanapanich, S., "High-Speed Compressible Flow Solutions by Adaptive Cell-Centered Upwinding Algorithm with Modified H-Correction Entropy Fix," *Advances in Engineering Software*, Vol. 34, No. 9, 2003, pp. 533–538.  
[https://doi.org/10.1016/S0965-9978\(03\)00083-8](https://doi.org/10.1016/S0965-9978(03)00083-8)
- [9] Sanders, R., Morano, E., and Druguet, M. C., "Multidimensional Dissipation for Upwind Schemes: Stability and Applications to Gas Dynamics," *Journal of Computational Physics*, Vol. 145, No. 2, 1998, pp. 511–537.  
<https://doi.org/10.1006/jcph.1998.6047>
- [10] Kemm, F., "A Carbuncle Free Roe-Type Solver for the Euler Equations," *Hyperbolic Problems: Theory, Numerics, Applications*, edited by S. Benzoni-Gavage, and D. Serre, Springer, Lyon, France, 2008, pp. 601–608.  
[https://doi.org/10.1007/978-3-540-75712-2\\_59](https://doi.org/10.1007/978-3-540-75712-2_59)
- [11] Ren, Y. X., "A Robust Shock-Capturing Scheme Based on Rotated Riemann Solvers," *Computers & Fluids*, Vol. 32, No. 10, 2003, pp. 1379–1403.  
[https://doi.org/10.1016/S0045-7930\(02\)00114-7](https://doi.org/10.1016/S0045-7930(02)00114-7)
- [12] Nishikawa, H., and Kitamura, K., "Very Simple, Carbuncle-Free, Boundary-Layer-Resolving, Rotated-Hybrid Riemann Solvers," *Journal of Computational Physics*, Vol. 227, No. 4, 2008, pp. 2560–2581.  
<https://doi.org/10.1016/j.jcp.2007.11.003>
- [13] Ren, X. D., Xu, K., Shyy, W., and Gu, C., "A Multi-Dimensional High-Order Discontinuous Galerkin Method Based on Gas Kinetic Theory for Viscous Flow Computations," *Journal of Computational Physics*, Vol. 292, July 2015, pp. 176–193.  
<https://doi.org/10.1016/j.jcp.2015.03.031>
- [14] Ren, X. D., Xu, K., and Shyy, W., "A Multi-Dimensional High-Order DG-ALE Method Based on Gas-Kinetic Theory with Application to Oscillating Airfoils," *Journal of Computational Physics*, Vol. 316, July 2016, pp. 700–720.  
<https://doi.org/10.1016/j.jcp.2016.04.028>
- [15] Ren, X. D., Xu, K., and Shyy, W., "A Gas-Kinetic Theory Based Multidimensional High-Order Method for the Compressible Navier-Stokes Solutions," *ACTA Mechanica Sinica*, Vol. 33, No. 4, Aug. 2017, pp. 733–741.  
<https://doi.org/10.1007/s10409-017-0695-2>
- [16] Liou, M. S., "Mass Flux Schemes and Connection to Shock Instability," *Journal of Computational Physics*, Vol. 160, No. 2, 2000, pp. 623–648.  
<https://doi.org/10.1006/jcph.2000.6478>
- [17] Ren, X. D., Gu, C. W., and Li, X. S., "Role of Momentum Interpolation Mechanism of the Roe Scheme in Shock Instability," *International Journal for Numerical Methods in Fluids*, Vol. 84, No. 6, 2017, pp. 335–351.  
<https://doi.org/10.1002/fld.v84.6>
- [18] Garnier, E., Mossi, M., Sagaut, P., Comte, P., and Deville, M., "On the Use of Shock-Capturing Schemes for Large-Eddy Simulation," *Journal of Computational Physics*, Vol. 153, No. 2, 1999, pp. 273–311.  
<https://doi.org/10.1006/jcph.1999.6268>
- [19] Li, X. S., and Li, X. L., "All-Speed Roe Scheme for the Large Eddy Simulation of Homogeneous Decaying Turbulence," *International Journal of Computational Fluid Dynamics*, Vol. 30, No. 1, 2016, pp. 69–78.  
<https://doi.org/10.1080/10618562.2016.1156095>
- [20] Weiss, J. M., and Smith, W. A., "Preconditioning Applied to Variable and Constant Density Flows," *AIAA Journal*, Vol. 33, No. 11, 1995, pp. 2050–2057.  
<https://doi.org/10.2514/3.12946>
- [21] Li, X. S., "Uniform Algorithm for All-Speed Shock-Capturing Schemes," *International Journal of Computational Fluid Dynamics*, Vol. 28, Nos. 6–10, 2014, pp. 329–338.  
<https://doi.org/10.1080/10618562.2014.936315>
- [22] Li, X. S., Gu, C. W., and Ren, X. D., "Cures for Expansion Shock and Shock Instability of Roe Scheme Based on Momentum Interpolation Mechanism," *Applied Mathematics and Mechanics (English Edition)*, Vol. 39, No. 4, 2018, pp. 455–466.  
<https://doi.org/10.1007/s10483-017-2283-8>

N. D. Sandham  
Associate Editor